FRACTAL ANALYSIS OF SURFACES COMPRISING HIERARCHICAL STRUCTURES

Ponomareva A.A.[1,2*], Moshnikov V.A.[1], Maraeva E.V.[1], Suchaneck G.[2]

[1] *St. Petersburg State Electrotechnical University (LETI), Prof. Popova 5, 197376 St. Petersburg, Russia*
[2] *TU Dresden Solid State Electronics Laboratory, 01062 Dresden, Germany*
**ap_k@inbox.ru*

Keywords: Hierarchical structures, atomic force microscopy, surface topography.

Abstract
In this work, we investigate the hierarchical surface topography evolution of sol-gel deposited SiO_2-SnO_2 nanocomposite films annealed in the temperature range of 200 to 600°C, reactive sputtered TiO_2 and $Pb(Zr,Ti)O_3$ nanocrystalline thin films and plasma-treated antireflective PET films by means of determining the fractal dimension and power spectral density (PSD) of surface topography recorded by atomic force microscopy (AFM). The PSDs of all samples were fitted to the K-correlation model (also called ABC model) of the PSD allowing a straightforward determination of RMS roughness, correlation length (grain size) and local fractal dimension

1 Introduction
A large number of modern electronic device applications are based on hierarchical micrometer- and nanometer-sized building blocks, for instance, metal oxide gas sensors, catalytic electrodes and electrolytes of solid oxide fuel cells, dye-sensitized solar cells, mesoporous films of biosensors, etc. Hierarchical meso- and nanoporous structures provide an effective liquid or gas transport via well aligned mesoporous structures and a large surface area for catalytic reactions [1]. In particular, gas sensitive composites based on tin dioxide are among the most promising materials to be used as fire detectors, leakage detectors, alarm devices warning the overcoming of threshold concentration values of hazardous gases in mines, controllers of ventilation in cars and planes etc [2]. Significant improvement of gas sensitivity and a reduction of the elevated operation temperatures can be achieved by using nanostructures exhibiting a characteristic size in order of the thickness of the surface space charge layer (several nanometers) [3]. For a fast sensor response, efficient analyte gas diffusion via a mesoporous structures is required toward the entire sensing surface. Thus, a tailored nanostructure should consist of hierarchical pore structures to provide simultaneously high gas sensitivity and fast sensor response.
Optical applications of hierarchical surface structures include the huge market of antireflective touch-screen and mobile phone coatings [4]. In this work, we evaluate the hierarchical surface topography evolution of oxide thin films and plasma-treated antireflective PET films by means of atomic force microscopy (AFM). Oxide samples include sol-gel derived SiO_2-SnO_2 nanocomposite films annealed in the temperature range of 200 to 600°C,

reactive sputtered TiO_2 and $Pb(Zr,Ti)O_3$ thin films. All samples exhibit a self-affine surface topography.

2 Theory

The structural characterization of hierarchical structures composed of lower dimensional building blocks requires application of different measurement techniques to cover a wide range of sizes being present within the microstructure. By taking advantage of the scaling property of many physical systems reducing the amount of data required for structural characterization, hierarchical structures might be adequately characterized by atomic force microscopy (AFM) with resolution from about 10 nm to the micrometer range. AFM provides already a digitized image suitable for numerical evaluation.
Surface topography is usually described in terms of surface roughness. Surface roughness is solely a function of height, that is, information about lateral topography is lost.
Power spectral density (PSD) is a technique that calculates power (roughness amplitude squared) as a function of spatial wavelengths k of the features that are contributing to the surface image. It is suitable for surfaces that can be well approximated by a series of sine waves. The slope of the log(*PSD*) vs log(k) plot at larger k values allows determination of the local roughness exponent α which characterizes the time behaviour of roughness evolution [5] enabling thus to analyze film growth. Thin film surfaces are known to be self affine, e.g., they are well modelled using anisotropic fractals and their topography is well described using the k-correlation model (also called ABC model) of the PSD yielding in the one-dimensional case (assuming perfectly isotropic surfaces) [6]

$$PSD = \frac{A}{(1+B^2k^2)^{C/2}} . \tag{1}$$

The PSD identifies wavelengths of features that contribute to the surface structure. It describes how the power of the Fourier transform of the surface height is distributed with wavenumber of the spatial frequency k in reciprocal space. The parameter A describes the low-frequency limit of the spectrum. The parameter B sets the point of the transition between the smooth low-frequency and fractal high-frequency behaviour of the PSD. It defines a correlation length beyond which the surface height fluctuations are not correlated thus representing a mean grain size. The parameter C gives a local fractal dimension which is valid for small spatial wavelengths of a self-affine surface [7, 8]. The integration of the PSD yields the RMS roughness σ of the surface

$${\sigma_{1-D}}^2 = \int_{f_{\min}}^{f_{\max}} PSD_{1-D}(k) \cdot dk . \tag{2}$$

3 Experimental

Nanocomposite SiO_2-SnO_2 thin films exhibiting high and stable gas sensitivities [9] were prepared by sol-gel technique [10]. Tin(II) chloride dihydrate $SnCl_2 \cdot 2H_2O$ was used as a tin precursor, tetraethylorthosilicate (TEOS) $C_8H_{20}O_4Si$ as a silica source and ethanol or *n*-butanol as solvents. The solutions were aged 24 h at room temperature. The sol was then spin-coated onto a glass substrate at 3000 revolutions per second for 30 seconds without an adhesion promoter. Annealing for 30 min was performed by transferring the samples immediately after spin coating into a muffle furnace heated to a temperature of 200, 300, 400, 500 and 600°C, respectively. XPS indicates that tin is in the tetravalent state. Film composition determined by XPS was in agreement with the Sn/(Sn+Si) ratio [9]. XRD revealed SnO_2 nanocrystals with a size of about 5 nm in an amorphous SiO_2 matrix.

Lead-zirconium-titanium oxide thin films were deposited by reactive sputtering from 8-inch Zr, Ti and Pb targets in an oxygen/argon atmosphere onto not intentionally heated, copper-coated Kapton® HN films by means of a LS730S multi-target sputtering system (Von Ardenne Anlagentechnik, Dresden) [11].The film composition was in rhombohedral range near the morphotropic phase boundary of the PZT phase diagram, e.g. at ratios $Zr/(Zr+Ti) > 0.52$ [12]. XRD revealed a nanocrystallite mixture of lead, zirconium and titanium oxides in the as-deposited films which can be transferred into perovskite $Pb(Zr,Ti)O_3$ by rapid temperature annealing. The value of the XRD Scherrer coherence length of PZT amounted to 36 nm, i.e. it is in the order of the domain width of PZT thin films and well above the size-limit for ferroelectricity.

TiO_2 thin films were deposited by reactive pulse magnetron sputtering in the transition mode between the metal and the oxide mode onto glass substrates using a pulse packet mode. Processing in the transition mode was stabilized by means of closed loop control of oxygen flow referencing to a Ti emission line (500 nm) in the low pressure plasma. Details of the deposition process are described elsewhere [13]. Samples consisting of different phases were selected for this investigation.

Polyethylene-terephtalate (PET Melinex®400 by Dupont Teijin Films) films were subjected to low-pressure plasma surface treatment in an argon-oxygen atmosphere as described in [4]. Stable self-organized nanostructures were created on these polymer substrates by using an ECR plasma source or a dual magnetron as an ion source driven in pure oxygen.

Microstructure of the samples was investigated by atomic force microscopy using an NTEGRA Therma scanning probe microscope (NT-MDT, Zelenograd, Russia). Tapping mode imaging was performed in air using silicon cantilevers (Type NSG01, NDT-MDT, Zelenograd, Russia). The two-dimensional AFM image was averaged over the profiles traced in fast scan direction using the Open Source Software Gwyddion 2.21 using Daniell (equal weight) window [14]. This allows reducing noise due to instrument drift appearing more pronounced in the slow scan direction. Moreover, the averaging over 256 scans is approximately equivalent to the integration of the two-dimensional PSD over the slow scan direction [15]. The fractal dimension of AFM images the films was determined by the cube counting method, the triangulation method and by means of the PSD slope at large wavenumbers [8]. RMS roughness, correlation lengths and local fractal dimension were derived from the fit to the model PSD.

The specific surface area (SSA) was measured using the Brunauer, Emmett and Teller (BET) method with nitrogen adsorption using a Sorbi-N4.1 instrument (ZAO META, Novosibirsk, Russia).

4 Results and Discussion

Figure 1 shows the PSDs of SiO_2-SnO_2 nanocomposites in dependence on annealing temperature. The corresponding fractal dimensions and PSD parameters are compiled in tables 1 and 2. The low-frequency region is not very well reproduced by the simplified model. On the one hand, this is attributed to not enough data points available in the averaging procedures so that an adequate statistics can not be obtained. On the other hand, in the special case of SiO_2-SnO_2 nanocomposites, micrometer sized pores are formed throughout the film bulk which provide an efficient analyte transport and which decrease sensor response and recovery time [10]. These macropores give additional contributions to the PSD which are not accounted in the model.

The fractal dimension of sol-gel deposited SiO_2-SnO_2 nanocomposites exhibits a maximum at about 400°C. It follows structure evolution including the formation of the porous structure by

solvent and water evaporation up to 400 °C, densification of the film above 400°C first by formation of a SiO_2 cage-like structure and SnO_2 crystallization above 500°C.

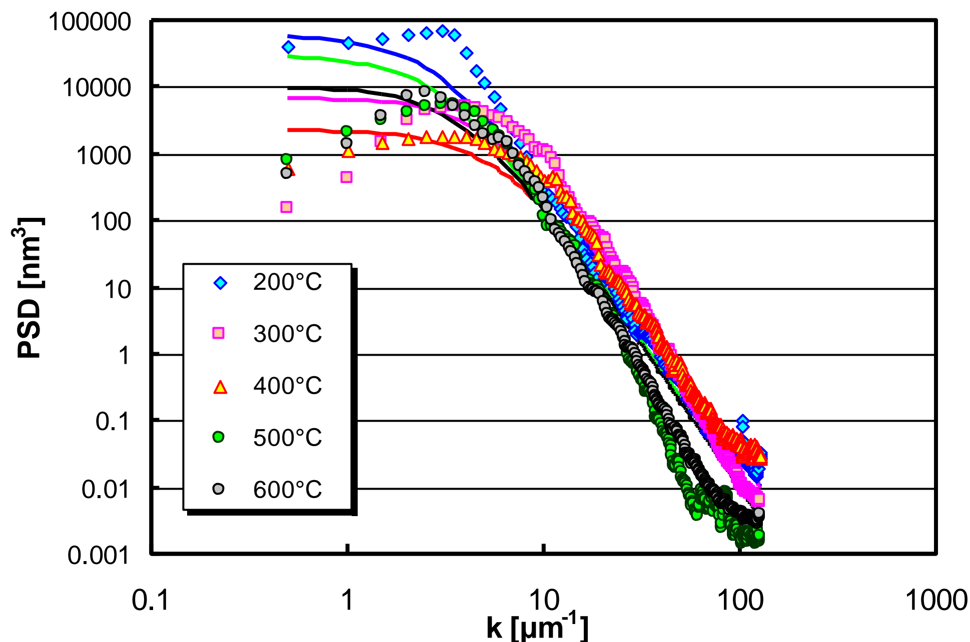

Figure 1. Power spectral density of the surface profile calculated from AFM images of SiO_2-SnO_2 nanocomposites in dependence on annealing temperature. The fit to the ABC model is shown by solid lines.

Annealing temperature, °C	Cube counting	Triangula-tion	PSD	RMS Roughness [nm]
200	2.15	2.21	1.95	29.6
300	2.16	2.22	1.85	13.8
400	2.26	2.38	2.1	7.02
500	2.17	2.21	1.9	35.5
600	2.14	2.18	1.85	12.5

Table 1. Fractal dimensions and RMS roughness of SiO_2-SnO_2 nanocomposites in dependence on annealing temperature [16].

Sample	*A* [µm³]	*B* [µm]	*C*
200	$6{\cdot}10^{-5}$	0.4	4.1
300	$7{\cdot}10^{-6}$	0.18	4.3
400	$2.3{\cdot}10^{-6}$	0.18	3.8
500	$3{\cdot}10^{-5}$	0.33	4.2
600	$1{\cdot}10^{-5}$	0.25	4.3

Table 2. k-correlation approximation (ABC-model) for SiO_2-SnO_2 nanocomposites in dependence on annealing temperature.

The PSD and fractal dimension of reactive sputtered lead-zirconium-titanium oxide thin films are strongly affected by processing conditions (Fig. 2, tables 3 and 4). Due to the absence of macropores, the description of the low frequency region of the PSD is improved. Here, substrate warpage should be additionally taken into account since the substrate was a polymer

film. Fractal dimensions are higher for films deposited under enhanced ion bombardment compared to standard films and lead-enriched ones.

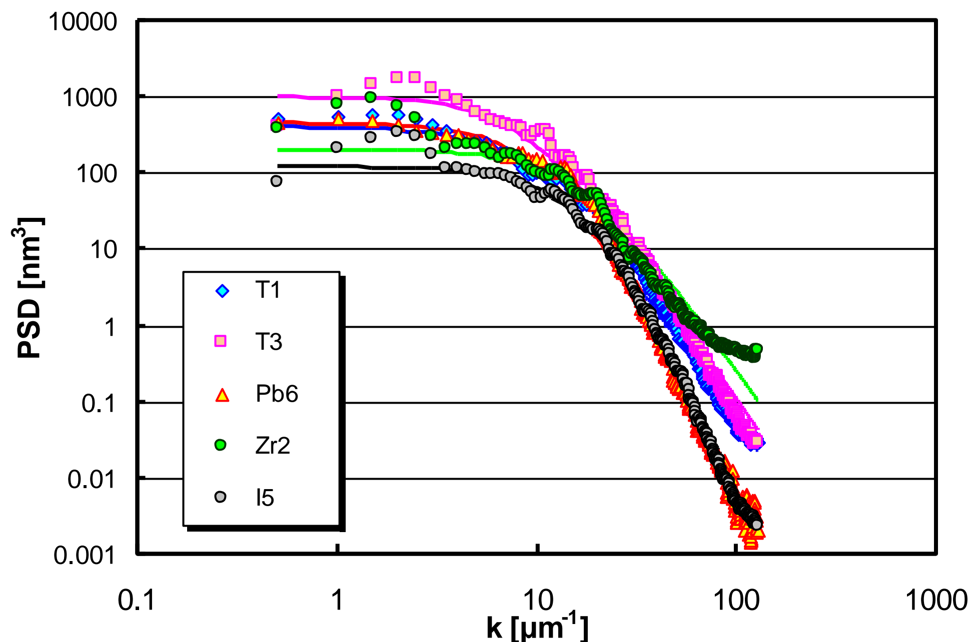

Figure 2. Power spectral density of the surface profile calculated from AFM images of reactive sputtered lead-zirconium-titanium oxide thin films. T1- DC-pulsed (100 kHz), T3 - DC-pulsed (300 kHz), Zr2 - high-power current pulse, I5 - high power current pulse with increased frequency, Pb6 - high power current pulse with increased lead excess. The fit to the ABC model is shown by solid lines.

Sample	Cube counting	Triangula-tion	PSD	RMS Roughness [nm]
T1	2.31	2.38	2.15	4.37
T3	2.31	2.41	2.1	7.63
Zr2	2.29	2.34	-	3.60
I5	2.39	2.48	2.15	3.31
Pb6	2.24	2.32	-	4.86

Table 3. Fractal dimensions and RMS roughness of lead-zirconium-titanium oxide thin films. Sample description is given in Fig. 2.

Sample	*A* [μm^3]	*B* [μm]	*C*
T1	$4 \cdot 10^{-7}$	0.11	3.7
T3	$1 \cdot 10^{-6}$	0.11	3.8
Zr2	$4.5 \cdot 10^{-7}$	0.08	5.5
I5	$2 \cdot 10^{-7}$	0.06	3.7
Pb6	$1.2 \cdot 10^{-7}$	0.05	6

Table 4. k-correlation approximation (ABC-model) of lead-zirconium-titanium oxide thin films. Sample description is given in Fig. 2.

The three TiO_2 samples selected for this research represent the rutile phase (substrate not intentionally heated during deposition), the anatase phase (substrate temperature during

deposition – 350°C) and a mixture of rutile and anatase phases (substrate temperature during deposition – 200°C). As expected, the last sample exhibits the highest roughness and correspondingly larger PSD values (Fig. 3 and table 5). The obtained PSD model parameters (cp. table 6) are in the order of that obtained earlier for titanium oxide films deposited onto glass substrates at 270 to 480 °C by d.c. magnetron-sputtering [17]. Here, water vapour was used as reactive gas and after deposition all samples were submitted to a thermal treatment. The thus deposited titanium oxide films had a polycrystalline, multiphase (anatase and/or rutile) structure. For pure rutile or anatase phases, we found a tendency to larger values $C > 4$ in this work giving evidence of shadowing and/or coarsening during film growth.

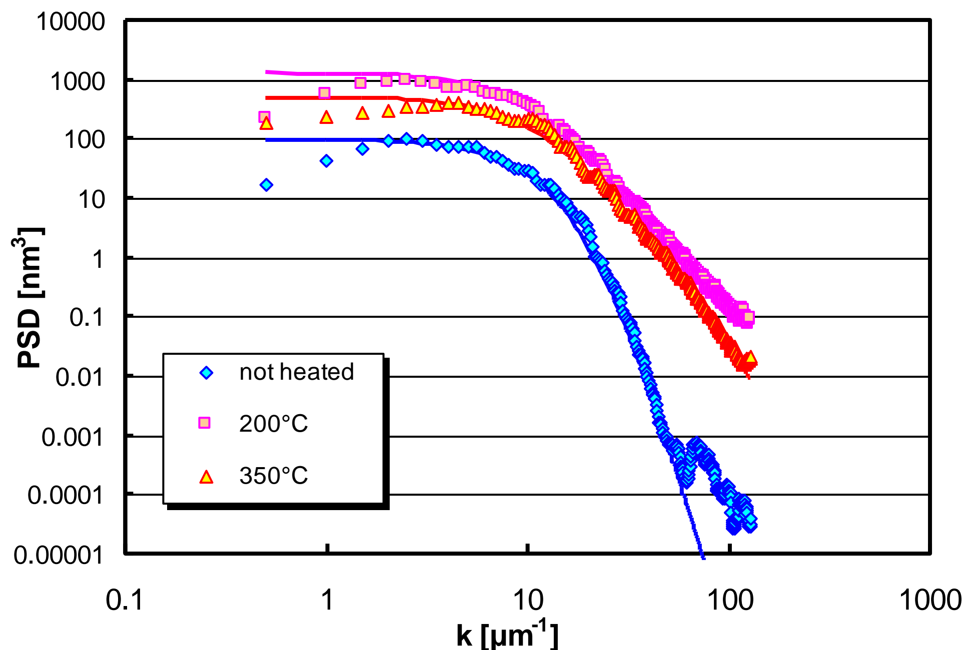

Figure 3. Power spectral density of the surface profile calculated from AFM images of reactive pulse magnetron sputtered TiO_2 films. The fit to the ABC model is shown by solid lines.

Sample	Cube counting	Triangula-tion	PSD	RMS Roughness [nm]
Not heated	2.31	2.4	–	2.1
200°C	2.31	2.41	2.2	7.1
350°C	2.37	2.44	1.7	5.2

Table 5. Fractal dimensions and RMS roughness of reactive pulse magnetron sputtered TiO_2 films.

Sample	*A* [µm³]	*B* [µm]	*C*
Not heated	$9.5 \cdot 10^{-8}$	0.05	(12)
200°C	$1.3 \cdot 10^{-6}$	0.11	3.6
350°C	$5.3 \cdot 10^{-7}$	0.08	4.7

Table 6. k-correlation approximation (ABC-model) of reactive pulse magnetron sputtered TiO_2 films.

The PSD, fractal dimensions and ABC model parameters of virgin and plasma treated PET films are summarized in figure 4 and tables 7 and 8. The initial waviness of PET films

disappears after plasma treatment. Both RMS roughness and fractal dimension increases in good agreement with an increase of the specific surface area determined by nitrogen absorption (BET) method.

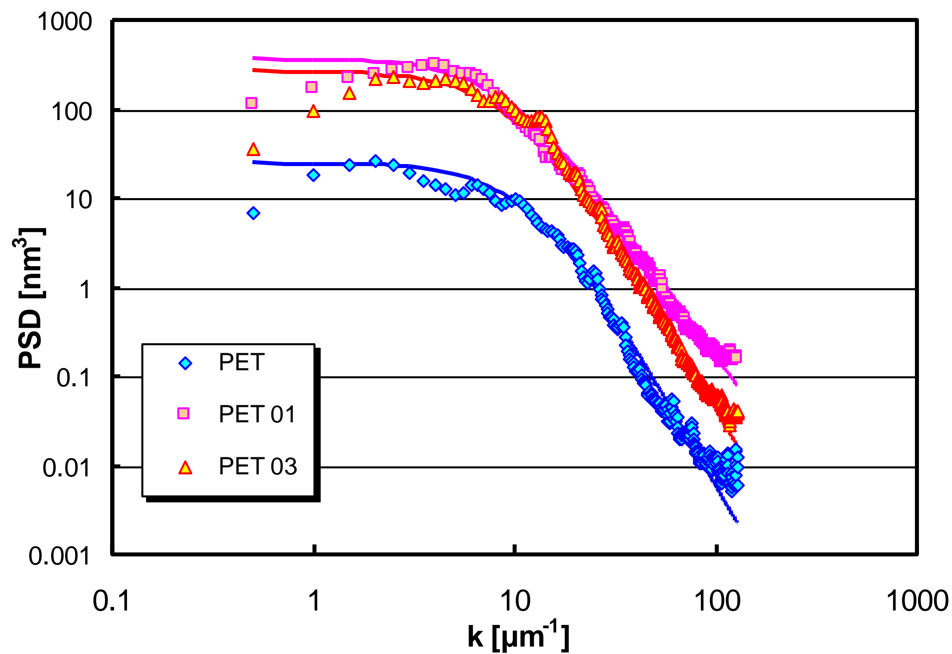

Figure 3. Power spectral density of the surface profile calculated from AFM images of PET samples.

Sample	Cube counting	Triangula-tion	PSD	RMS Roughness [nm]	Specific surface area [m^2/g]
PET (virgin)	2.30	2.36	2	1.24	0.1 ± 0.03
PET 01	2.39	2.49	2.4	4.18	0.2 ± 0.04
PET 03	2.36	2.48	2.1	3.73	0.7 ± 0.55

Table 7. Fractal dimensions of plasma treated PET samples. The virgin PET substrate values are given for comparison.

Sample	*A* [µm^3]	*B* [µm]	*C*
PET (virgin)	$2.5 \cdot 10^{-8}$	0.08	4.0
PET 01	$3.7 \cdot 10^{-7}$	0.11	3.2
PET 03	$2.7 \cdot 10^{-7}$	0.10	3.8

Table 8. k-correlation approximation (ABC-model) of plasma treated samples. The virgin PET substrate values are given for comparison.

Conclusions

In this work we have demonstrated that the local fractal dimension determined from AFM images is an appropriate and easy to use tool for the characterization of hierarchical nanostructures. With regard to the finite numbers of pixels of an AFM image, the triangulation method provides more reliable values of fractal dimension while the PSD allows analysis of substrate waviness and film growth.

Acknowledgements
This work was supported by supported by contracts 16.740.11.0211, P399 and P2279 of the Federal Target Program "Scientific and Scientific-Pedagogical Personnel of Innovative Russia for the period 2009-2013", and by the Erasmus Mundus External Co-operation Window Programme of the European Union (A.P.).

References

[1] Lee J.-H. Gas sensors using hierarchical and hollow oxide nanostructures: Overview. *Sensors and Actuators B,* **140,** pp. 319‑336 (2009).
[2] Korotcenkov G. Metal oxides for solid-state gas sensors: What determines our choice? *Materials Science and Engineering B*, **139**, pp. 1–23 (2007).
[3] Xu C., Tamaki J., Miura N., Yamazoe N. Grain size effects on gas sensitivity of porous SnO_2-based elements. *Sensors and Actuators B,* **3**, pp. 147-155 (1991).
[4] Schönberger W., Gerlach G., Fahland M., Munzert P., Schulz U., Thielsch R., Kleinhempel R. Large-area fabrication of stochastic nano-structures on polymer webs by ion- and plasma treatment. *Surface and Coatings Technology*, **205**, pp. S495-S497 (2011).
[5] Viscek T. *Fractal Growth Phenomena*, 2nd. Edition, Singapore: World Scientific (1992).
[6] Church E.L., Takacz P.Z. The optimal estimation of finish parameters, *Proc. SPIE*, **1530**, pp. 71-85 (1991).
[7] Douketis C., Wang Z., Haslett T.L., Moskovits M. Fractal character of cold-deposited silver films determined by low-temperature scanning tunneling microscopy, *Phys. Rev. B*, **51**, pp. 11022-11031 (1995).
[8] Mandelbrot B.B., Passoja D.E., Paullay A.J. Fractal character of fracture surfaces of metals, *Nature*, **308**, pp. 721-722 (1984).
[9] Ponomareva A.A., Moshnikov V.A., Glöß D., Delan A., Kleiner A., Suchaneck G. Metal-oxide-based nanocomposites comprising advanced gas sensing properties. *J. Phys. Conf. Ser*, **345,** 012029 (2012).
[10] Ponomareva A.A., Moshnikov V.A., Suchaneck G. Mesoporous sol-gel deposited SiO_2-SnO_2 nanocomposite thin films. *IOP Conf. Ser.: Mater. Sci. Eng.*, **30**, 012003 (2012).
[11] Kleiner A., Suchaneck G., Adolphi B., Ponomareva A., Gerlach G. PZT thin films deposited on copper-coated polymer film substrates. *Ferroelectrics* (2012) DOI:10.1080/00150193.2012.676961.
[12] Jaffe B., Cook W., Jaffe H. *Piezoelectric Ceramics.* Academic Press, New York, (1971).
[13] Glöß D., Frach P., Zywitzki O., Modes T., Klinkenberg S., Gottfried C. Photocatalytic titanium dioxide thin films prepared by reactive pulse magnetron sputtering at low temperature. *Surf. Coat. Technol*. **200**, pp. 967–971 (2005).
[14] Gwyddion – data analysis software: http://gwyddion.net
[15] Marx E., Malik I. J., Strausser Y. E., Bristow T., Poduje N., Stover J. C. Power spectral densities: A multiple technique study of different Si wafer surfaces. *J. Vac. Sci. Technol. B*, **20**, pp. 31-41 (2002).
[16] Ponomareva A.A., Moshnikov V.A., Suchaneck G. The influence of thermal annealing on the fractal dimension of the surface of sol-gel SiO_2-SnO_2 films. *Mater. Sci. Trans.* **15**, pp. 45-48 (2011).
[17] Gavrila R., Dinescu A., Mardare D. A power spectral density study of thin films morphology based on AFM profiling. *Roman. J. Inf. Sci. Technol.,* **10**, pp. 291-300 (2007).